IRAQI JOURNAL OF MATERIALS
Volume (4) Issue (1) January-March 2025, pp. 3-8

Nitrogen-Doped Titanium Dioxide and Cobalt Oxide Thin Films Prepared by Reactive Sputtering

Noor Alhuda H. Hashim [1], Firas J. Kadhim [2], Zinah S. Abdulsattar [2]

[1] *Uruk University College, Baghdad, IRAQ*
[2] *Department of Physics, Faculty of Science, University of Baghdad, Baghdad, IRAQ*

Abstract

In the present work, reactive sputtering technique was used to prepare layers of nitrogen-doped titanium dioxide (TiO_2) and cobalt oxide (Co_3O_4) thin films on indium-tin oxide (ITO). Both materials showed polycrystalline structures. The Co_3O_4 samples showed polygon-shaped particles with apparent aggregation, while the TiO_2 samples showed approximately spherical particles with lower minimum size when compared to that of Co_3O_4 samples. The absorption of Co_3O_4 films was very sensitive to the variation of oxygen content in the gas mixture as the absorbance increased with increasing the oxygen in the gas mixture due to the increase in formation of the Co_3O_4 molecules. Energy band gap was shown dependent on the preparation conditions.

Keywords: Electrochromism; Photoelectrochromic devices; Titanium dioxide; Cobalt oxide
Received: 20 August 2024; **Revised:** 22 October 2024; **Accepted:** 29 October; **Published:** 1 January 2025

1. Introduction

In the last years, smart windows have gained considerable attention by the international scientific community due to significant energy savings [1]. The phenomenon of color change by chromic materials due to external stimuli, such as electric field, pressure, light, ions, solvent, etc., is called chromism. Chromic materials change the optical properties like transmission, reflectance, absorption, and emittance due to these external stimuli [2]. Electrochromism is the phenomenon exhibited by electrochromic materials that change color when an electric potential is applied [3-4]. While Photoelectrochromism is also the phenomena of changing color of chemical compounds induced by electrochemical oxidation and reduction, under the effect of a variation an electric voltage and/or in the intensity of a light radiation [6]. This chromic effect can be put to practical use in the design of “Smart Window”, smart windows that can control the amount of light passing through it based on EC materials [7]. These EC materials are mainly classified into two categories: anodic and cathodic materials [8,9], anodic EC materials, which are coloring under ion extraction “oxidation process” and cathodic EC materials, which are coloring under ion insertion “reduction process” [10]. The inorganic EC materials have a good electrochemical reversibility, chemical stability and high coloring efficiency where organic EC materials display poor durability [11-13]. Titanium dioxide (TiO_2) is an n-type semiconducting material that has superior properties such as non-toxic, high stability and strong oxidizing agent (with large surface area) has very high photocatalytic activity [14-16]. Due to these properties this material has been applied in various applications such as solar cells, sensors, environmental remediation and as cathodic material of electrochromic devices [17]. As titanium dioxide does not absorb visible light, there is several methods to overcome this problem including the doping with non-metallic elements such as nitrogen [18-19]. Cobalt oxide (Co_3O_4) is one of the most important metal oxides, p-type antiferromagnetic semiconductor with direct band gap between 1.48-2.19 eV [20,21]. This oxide has a wide range of applications due optical, magnetic, electronic, chemical, electrochemical and mechanical properties [22-24]. The preparation and characterization of cobalt oxides Co_3O_4 have been extensively studied due to attractive applications in solar cells, catalysis, batteries, corrosion protective coatings, magnetic nanostructures and magnetic storage systems, electrochromic EC devices. Co_3O_4 has been reported to be a good anodic coloration material for the EC application [25,26]. There are several deposition techniques to prepare oxide thin films such as sputtering, spray pyrolysis, chemical vapor deposition, pulsed laser deposition, electrophoretic deposition, sol-gel process, etc. [27-29]. DC reactive magnetron sputtering technique was employed for the preparation of the EC thin films because it

provides high purity, high homogeneity and good control of the structural phase of the deposited film by controlling the gas mixing ratio [30].

In this work, the layers of electrochromic and photoelectrochromic device based on N-doped TiO_2 and Co_3O_4 oxides are prepared by dc reactive magnetron sputtering technique. The optical and structural characteristics of each layers will be studied and optimized to synthesis single layer configuration for ECD and multi-layers configuration for PECD devices and compared coloring-bleaching response for each configurations.

2. Experimental Details

Cobalt oxide was prepared by using dc reactive magnetron sputtering and more information about the preparing conditions of cobalt oxide may be obtained elsewhere [31,32]. A high-purity titanium sheet with 60 mm diameter and 0.5 mm thickness was mounted on the cathode and glass substrate placed on a heat sink was placed on the anode. The optimum preparation conditions include discharge voltage of 2.5 kV and discharge current of 45 mA, while the distance between the target and the substrate was fixed at 4 cm. N-doped TiO_2 thin films were prepared using different $Ar:O_2:N_2$ gas mixing ratios (40:40:20, 60:30:10: 43:42:15 and 76:19:5) and deposition time of 3 hours.0

3. Results and Discussion

The crystal structure of the Co_3O_4 thin film prepared using $Ar:O_2$ gas mixing ratio of 60:40 was investigated by an X-ray Shimadzu Diffractometer using Cu-Kα source (1.54Å). The XRD pattern shows the diffraction peaks which indicate that the crystalline structure of these films constitutes a single phase of Co_3O_4 with a spinel-type structure. The XRD pattern in Fig. (1) shows a major peak at about 37° corresponding to crystal plane of (311). This peak has the highest intensity, indicating the oriented growth of the sample in the (311) direction. Six peaks observed at 31.5°, 37.1°, 38.7°, 45.0°, 55.9°, 59.6°, 65.4° and 77.7° are corresponding to (220), (311), (222), (400), (422), (511), (440) and (533) planes, which indicate the formation of pure Co_3O_4 [33].

Figure (2) shows the XRD pattern of N-doped TiO_2 thin film prepared using $Ar:O_2:N_2$ gas mixing ratio of 40:40:20 after 3 hours of deposition time with heat sink under the substrate. The diffraction peaks observed at 22.4°, 38.5°, 53.1°, 63.2°, 70.7°,76.3° and 77.9° are assigned to A(101), A(104), A(105), A(204), A(220), A(215) and A(206) planes of anatase phase, respectively. Other peaks observed at 35.3° and 42.1° are corresponding to TiN(111) and TiN(200) according to JCPDS card no. 38-1420 [34]. The diffraction peaks assigned at 36.2° and 40.3° corresponding to crystal planes (101) and (111) were confirmed for the rutile phase according to JCPDS card no. 88-1175 [35]. No peaks belonging to other compounds or impurities were observed, which can be considered as an advantage of the sputtering technique used in this work and the fine control of gas mixing ratio.

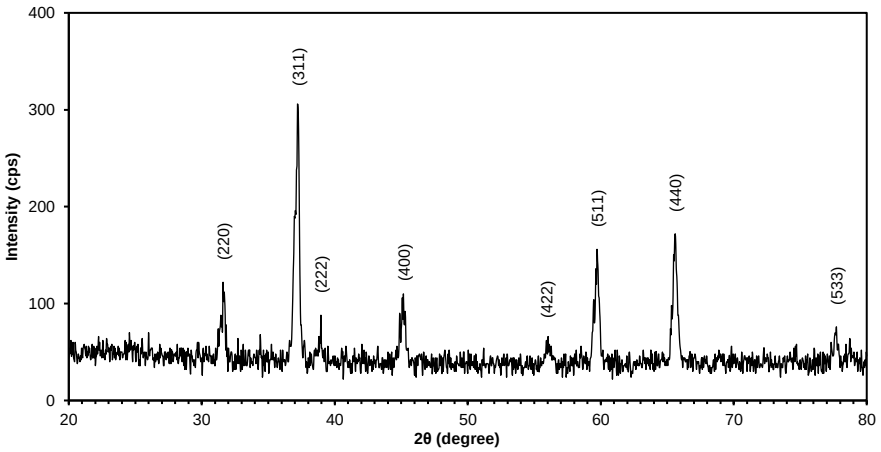

Fig. (1) XRD pattern of Co_3O_4 thin film using gas mixing ratio 60:40

The nanoparticle size of the synthesized nanostructured layers were studied by field-emission scanning electron microscopy (FE-SEM). The image in Fig. (3a) with scale of 500 nm shows that the Co_3O_4 nanoparticles are spherical with minimum particle size of 37.32 nm, while the image in Fig. (3b) with the same scale shows the N-doped TiO_2 nanoparticles with minimum particle size of 28.09 nm. The aggregated particles indicates good connectivity between these nanoparticles. The nanoparticles can form complex assemblies referred as aggregates, which typically consist of particles in the nanoscale (5-50 nm). They are held together by weak forces arising from the van der Waals force, which leads to an electrostatics effect through the residual charge of the structure. Ambient humidity plays an important

 ISSN (print) 2958-8960 (online) 3006-6042 Printed in IRAQ

role in determining the fundamental mechanical response and dynamics of these assemblies [36]. The FE-SEM image indicates that the prepared nanoparticles are uniformly distributed. This type of morphology is beneficial to use these nanostructures for EC and PEC devices and supercapacitor application [37,38].

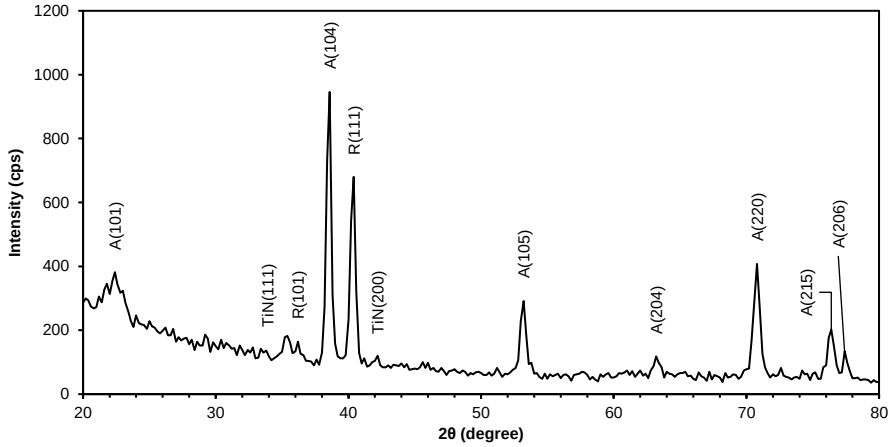

Fig. (2) XRD pattern of N-doped TiO_2 thin film prepared using gas mixing ratio of 40:40:20

Figure (4) shows the FTIR spectrum recorded in the range 400-4000 cm^{-1} for the Co_3O_4 sample prepared using gas mixing ratio of 60:40 after deposition time of 1 hour. Two strong peaks were observed, the first at 572.82 cm^{-1} was assigned to Co-O stretching vibration mode, in which Co^{3+} is octahedrally coordinated, and the second peak at 663.47 cm^{-1} was assigned to bridging vibration, in which Co^{2+} is tetrahedrally coordinated [39]. This further confirms the formation of Co_3O_4. The peaks seen at 1571.88 and 3436.91 cm^{-1} are ascribed to the OH stretching and bending modes, respectively, of water adsorbed by the Co_3O_4 sample. The peaks at 2408.93 and 1423.37 cm^{-1} are characteristic of asymmetric vibrations of CO_2 and CO^{-2}, respectively, which were also adsorbed from the air [40].

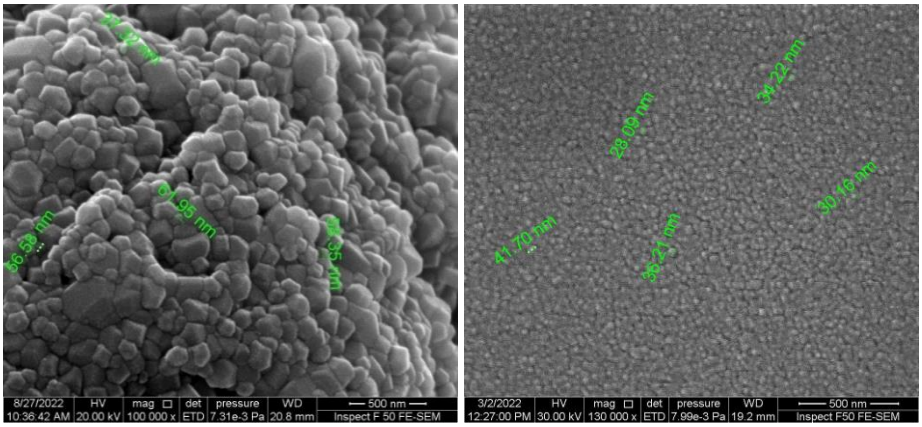

(a) **(b)**

Fig. (3) FE-SEM images of (a) Co_3O_4 sample prepared using 60:40 gas mixing ratio, and (b) N-doped TiO_2 sample prepared using 40:40:20 gas mixing ratio

For the N-doped TiO_2 sample prepared using gas mixing ratio of 40:40:20 after deposition time of 3 hours, the peak seen at 408.91 cm^{-1} is assigned to Ti-O-Ti bonds in the TiO_2 lattice, while the bands ascribed to Ti-O symmetric and asymmetric stretching vibration modes were observed around 447 and 667 cm^{-1}, respectively. The band at 870 cm^{-1} can be ascribed to the vibration of surface absorbed N-O, whereas the Ti-N vibration bands can be observed at around 1250 cm^{-1} in the range of 1080-1474 cm^{-1} [41,42]. The peak at 3450 cm^{-1} is attributed to the stretching and bending vibration of the OH group in water molecules in the atmosphere [43].

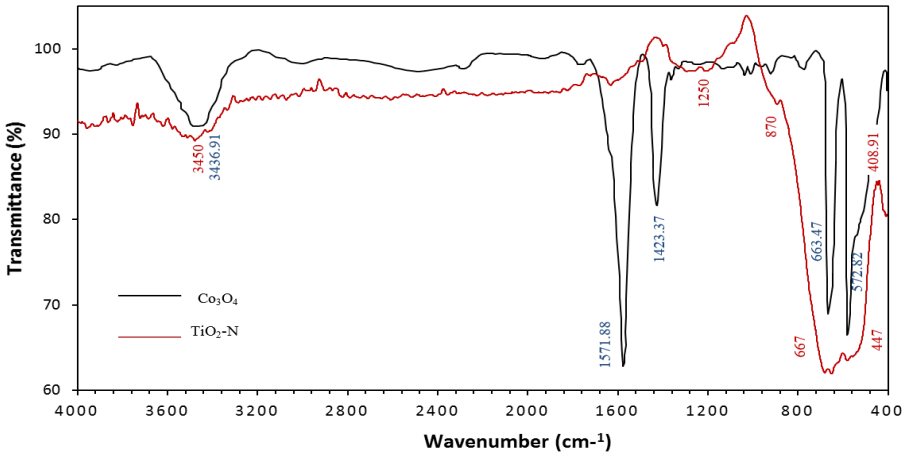

Fig. (4) FTIR spectra of Co_3O_4 sample prepared using gas mixing ratio 60:40 and N-doped TiO_2 sample prepared using gas mixing ratio 40:40:20

The UV-visible absorption spectra within the spectra range of 400-700nm for the Co_3O_4 thin films prepared using different gas mixing ratios are shown in Fig. (5). The absorbance is increasing with increasing oxygen content in the gas mixture and this may be attributed to the formation of more Co_3O_4 nanoparticles. Also, due to increasing oxygen content in the gas mixture, the measurements show very slight blue shift in the absorption edge towards shorter wavelengths [44]. The weak absorption band around 650 nm can be ascribed to the band gap energy transition $p(O^{2-})\rightarrow t_2(Co^{2+})$ [45].

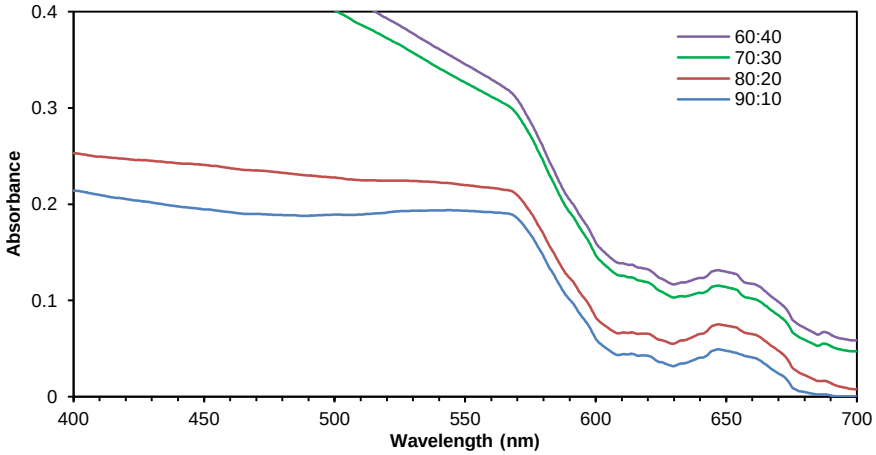

Fig. (5) Absorption spectra of Co_3O_4 thin films prepared by using different gas mixing ratios

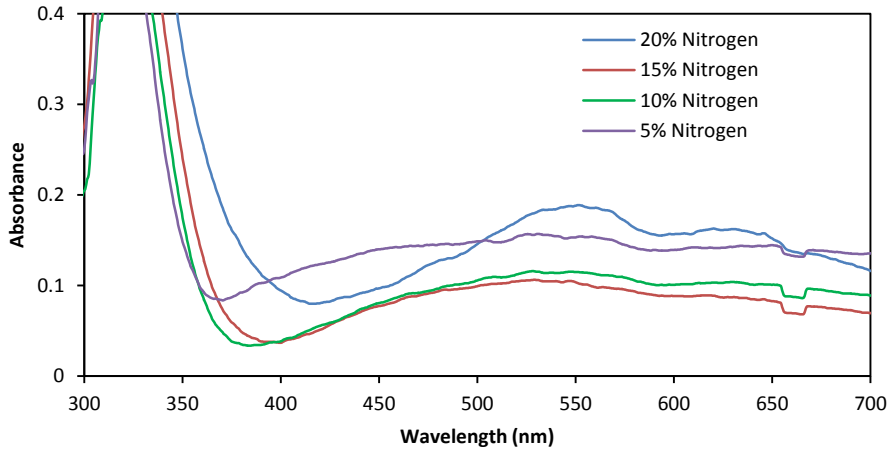

Fig. (6) Absorption spectra of N-doped TiO_2 thin films prepared using different concentrations of nitrogen in the gas mixture

ISSN (print) 2958-8960 (online) 3006-6042 Printed in IRAQ

The absorption spectra within the spectral range of 300-700 nm for the N-doped TiO_2 thin films prepared using different doping concentrations of nitrogen are shown in Fig. (6). It is clear that the optical absorption edges are shifted towards longer wavelength (red shift) by increasing the concentration of nitrogen, as they interstitially occupy some positions of oxygen in the TiO_2 lattice [46,47].

The Tauc's equation can be used to determine the energy band gap from the relationship between the photon energy and absorption coefficient as [48]:

$$(\alpha h\nu)^n = A(h\nu - E_g) \qquad (2)$$

where *A* is a constant, E_g is the energy band gap and n is a constant, taking values of 0.5 or 2 for indirect and direct allowed transitions, respectively

In accordance to the results of absorption, figure (7a) shows that the energy band gap of Co_3O_4 thin film prepared by using 60:40 gas mixing ratio and 1 hour of deposition time is 2.15 eV [49], while figure (7b) shows the energy band gap of N-doped TiO_2 thin films prepared using different concentrations of nitrogen (5, 10, 15 and 20%). The energy band gap was shifted to lower energies and decreased to 2.94 eV due to the contribution of nitrogen dopants in TiO_2 nanostructures. The lowest value of E_g was obtained for the sample doped with the highest concentration of nitrogen (20%) as its values were 3.03, 3.12 and 3.17 eV for concentrations of 15, 10 and 5%, respectively.

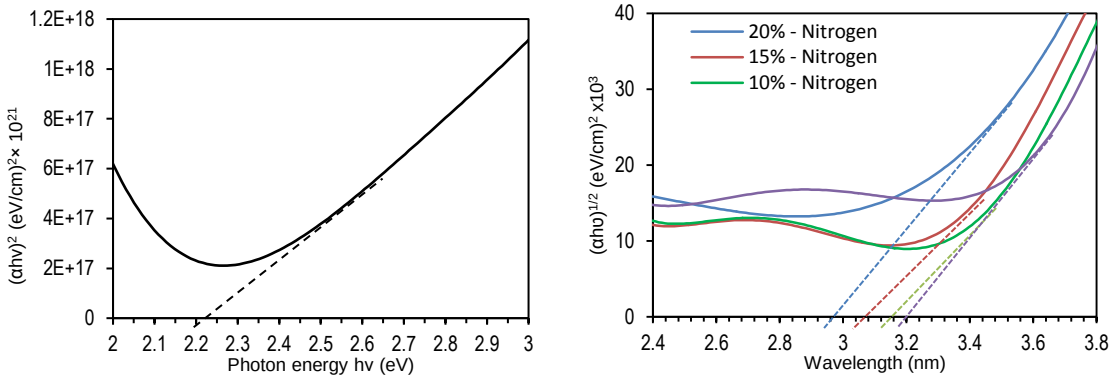

(a) **(b)**

Fig. (7) Determination of energy band gap for (a) Co_3O_4 sample prepared using gas mixing ratio of 60:40, and (b) N-doped TiO_2 samples using different concentrations of nitrogen in the gas mixture

4. Conclusion

In the present work, reactive sputtering technique was used to prepare layers of nitrogen-doped titanium dioxide (TiO_2) and cobalt oxide (Co_3O_4) thin films on indium-tin oxide (ITO). Both materials showed polycrystalline structures. The Co_3O_4 samples showed polygon-shaped particles with apparent aggregation, while the TiO_2 samples showed approximately spherical particles with lower minimum size when compared to that of Co_3O_4 samples. The absorption of Co_3O_4 films was very sensitive to the variation of oxygen content in the gas mixture as the absorbance increased with increasing the oxygen in the gas mixture due to the increase in formation of the Co_3O_4 molecules. Energy band gap was shown dependent on the preparation conditions.

References

[1] A. Dokouzis et al., "Photoelectrochromic devices with cobalt redox electrolytes", *Materials Today: Energy*, 15 (2020) 100365.
[2] O.A. Hamadi and K.Z. Yahiya, "Optical and electrical properties of selenium-antimony heterojunction formed on silicon substrate", *Sharjah Univ. J. Pure Appl. Sci.*, 4(2) (2007) 1-11.
[3] J. Mardaljevic, R. K. Waskett and B. Painter, "Electrochromic Glazing in Buildings: A Case Study", in **"Electrochromic Materials and Devices"**, Wiley-VCH Verlag GmbH (2013) 571–592.
[4] C. Costa et al., "Photoelectrochromic devices: Influence of device architecture and electrolyte composition", *Electrochimica Acta*, 219 (2016) 99-106.
[5] K.-D. Li, P.-W. Chen and K.-S. Chang, "Low-Temperature Deposition of Transparent Conducting Films Applied to Flexible Electrochromic Devices", *Materials*, 14(17) (2021) 4959.
[6] Z.S. Abdulsattar and F.J. Kadhim, "Synthesis and Characteristics of Electrochromic Glass with Multi-Layer Configuration Based on glass/ITO/WO_3/ZrO_2/NiO/ITO/glass", *Iraqi J. Appl. Phys.*, 15(4) (2019) 17-22.
[7] P. Bonhote, L. Walder and M. Gratzel, "Electrochromic or photoelectrochromic device", US Patent, No. 6734305, May 2004.
[8] X. Wu, J. Zheng and C. Xu, "Highly Optical Performance Photoelectrochromic Device Based on Br^-/Br_3^- Electrolyte", *Electrochimica Acta*, 191 (2016) 902-907.
[9] M.A. Bhatt and A.R. Tanna, "A Review on Electrochromic Materials for Smart Window Applications: Past, Present and Future", Int. Res. Conf. on Innov. Startup and Invest. (ICOSTART-2019) (Rajkut, India) September 2020.
[10] W. Zhang et al., "Nanostructured inorganic electrochromic materials for light applications", *Nanophot.*, 10(2) (2020) 825-850.
[11] B. Li et al., "Recent Advances in Inorganic Electrochromic Materials from Synthesis to Applications: Critical Review on Functional Chemistry and Structure Engineering", *Chemistry - An Asian J.*, 17 (2022) e202200022.

[12] S.-I. Park et al., "A review on fabrication processes for electrochromic devices", *Int. J. Precis. Eng. Manuf. Green Technol.*, 3(4) (2016) 397-421.
[13] F.J. Al-Maliki, O.A. Hammadi and E.A. Al-Oubidy, "Optimization of Rutile/Anatase Ratio in Titanium Dioxide Nanostructures prepared by DC Magnetron Sputtering Technique", *Iraqi J. Sci.*, 60(special issue) (2019) 91-98.
[14] O.A. Hamadi, B.A.M. Bader and A.K. Yousif, "Electrical Characteristics of Silicon p-n Junction Solar Cells Produced by Plasma-Assisted Matrix Etching Technique", *Eng. Technol. J.*, 28 (2008).
[15] E.L. Runnerstrom et al., "Nanostructured electrochromic smart windows: Traditional materials and NIR-selective plasmonic nanocrystals", *Chem. Commun.*, 50(73) (2014) 10555-10572.
[16] O. Carp, C.L. Huisman and A. Reller, "Photoinduced reactivity of titanium dioxide", *Prog. in Solid State Chem.*, 32 (2004) 33-117.
[17] M.A. Aziz and F.J. Kadhim, "Characteristics of Multilayer glass/ITO/N:TiO_2/NiO/KOH/Pt/glass Photoelectrochromic Device Synthesized by Reactive Magnetron Sputtering", *Iraqi J. Appl. Phys.*, 18(3) (2022) 11-17.
[18] F.J. Kadhim, O.A. Hammadi and N.H. Mutesher, "Photocatalytic activity of TiO_2/SiO_2 nanocomposites synthesized by reactive magnetron sputtering technique", *J. Nanophot.*, 16(2) (2022) 026005 DOI: 10.1117/1.JNP.16.026005
[19] O.A. Hammadi, "Effects of Extraction Parameters on Particle Size of Titanium Dioxide Nanopowders Prepared by Physical Vapor Deposition Technique", *Plasmonics*, 15(6) (2020) 1747-1754.
[20] V. Patil et al., "Synthesis and Characterization of Co_3O_4 Thin Film", *Soft Nanosci. Lett.*, 2(1) (2012) 1-7.
[21] A.E. Kaloyeros et al., "Review–cobalt thin films: trends in processing technologies and emerging applications", *ECS J. Solid State Sci. Technol.*, 8 (2019) 119-152.
[22] L.D. Kadam, S.H. Pawar and P.S. Patil, "Studies on ionic intercalation properties of cobalt oxide thin films prepared by spray pyrolysis technique", *Mater. Chem. Phys.*, 68(1-3) (2001) 280-282.
[23] L. Li et al., "Low Ni-doped Co_3O_4 porous nanoplates for enhanced hydrogen and oxygen evolution reaction", *J. Alloys Comp.*, 823 (2020) 153750.
[24] P.N. Shelke et al., "Synthesis, characterization and optical properties of selective Co_3O_4 films 1-D interlinked nanowires prepared by spray pyrolysis technique", *Fuel*, 112 (2013) 542-549.
[25] R. Drasovean, S. Condurache-Bota and N. Tigau, "Structural and electrical characterization of cobalt oxide semiconductors", *J. Sci. Arts*, 2(13) (2010) 379-384.
[26] F.J. Al-Maliki, O.A. Hammadi, B.T. Chiad and E.A. Al-Oubidy, "Enhanced photocatalytic activity of Ag-doped TiO_2 nanoparticles synthesized by DC Reactive Magnetron Co-Sputtering Technique", *Opt. Quantum Electron.*, 52 (2020) 188.
[27] R. Hippler et al., "Deposition of cobalt oxide films by reactive pulsed magnetron sputtering", *Surf. Coat. Technol.*, 405 (2021) 126590.
[28] J. Alami, "Plasma Characterization and Thin Film Growth and Analysis in Highly Ionized Magnetron Sputtering", Linköping Studies in Sci. Technol., Diss. No. 948 (2005) ISBN 91-85299-40-5.
[29] O.A. Hammadi and N.E. Naji, "Fabrication and Characterization of Polycrystalline Nickel Cobaltite Nanostructures Prepared by Plasma Sputtering as Gas Sensor", *Phot. Sen.*, 8(1) (2018) 43-47.
[30] N.H. Hashim and F.J. Kadhim, "Structural and Optical Characteristics of Co_3O_4 Nanostructures Prepared By DC Reactive Magnetron Sputtering", *Iraqi J. Appl. Phys.*, 18(4) (2022) 31-36.
[31] H.E. Swnason et al., "Standard X-Ray Diffraction Powder Patterns", International Center for Diffraction Data (ICDD) (Washington DC, 1971), NBS monograph 25, Sec. 9, p. 29
[32] K. Thamaphat, P. Limsuwan and B. Ngotawornchai, "Phase Characterization of TiO_2 Powder by XRD and TEM", *Kasetsart J. (Nat. Sci.)*, 42 (2008) 357-361.
[33] C. Li et al., "*in situ* growth of TiO_2 on TiN nanoparticles for nonnoble-metal plasmonic photocatalysis", *RSC Advances*, 6 (2016) 72659-72669.
[34] S.C. Endres, L.C. Ciacch and L. Madler, "A review of contact force models between nanoparticles in agglomerates, aggregates and films", *J. Aerosol Sci.*, 153 (2021) 105719.
[35] R. Lakra et al., "Synthesis and characterization of cobalt oxide (Co_3O_4) nanoparticles", *Mater. Today: Proc.*, 2 September 2020, 269-271.
[36] O.A. Hamadi, "The fundamentals of plasma-assisted CVD technique employed in thin films production", *Iraqi J. Appl. Phys. Lett.*, 1(2) (2008) 3-8.
[37] A. Hodaei, A.S. Dezfuli and H.R. Naderi, "A high-performance supercapacitor based on N-doped TiO_2 nanoparticles", *J. Mater. Sci.: Materials in Electronics*, 29 (2018) 14596-14604.
[38] K. Maaz, **"Cobalt"**, InTech Open (Croatia, 2017), Ch. 4, p. 56.
[39] A.N. Naveen and S. Selladurai, "Investigation on physiochemical properties of Mn substituted spinel cobalt oxide for supercapacitor applications", *Electrochimica Acta*, 125 (2014) 404-414.
[40] Asraa M. Hameed and Mohammed A. Hameed, "Highly-Pure Nanostructured Metal Oxide Multilayer Structure Prepared by DC Reactive Magnetron Sputtering Technique", *Iraqi J. Appl. Phys.*, 18(4) (2022) 9-14.
[41] Y. Huo et al., "Highly active $TiO_{2-x-y}N_xF_y$ visible photocatalyst prepared under supercritical conditions in NH_4F/EtOH fluid", *Appl. Catal. B, Environ.*, 89(3-4) (2009) 543-550.
[42] F.J. Al-Maliki and N.H. Al-Lamey, "Synthesis of Tb-doped titanium dioxide nanostructures by sol– gel method for environmental photocatalysis applications", *J. Sol-Gel Sci. Technol.*, 81 (2017) 276-283.
[43] S. Baset et al., "Size measurement of metal and semiconductor nanoparticles via UV-vis absorption spectra", *Dig. J. Nanomater. Biostruct.*, 6(1) (2011) 1-8.
[44] W.M. Haynes, **"CRC Handbook of Chemistry and Physics"**, 92nd ed., Taylor & Francis Group (NY, 2012), Ch. 10, pp. 93-146.
[45] O.A. Hammadi, F.J. AL-Maliki and E.A. Al-Oubidy, "Photocatalytic Activity of Nitrogen-Doped Titanium Dioxide Nanostructures Synthesized by DC Reactive Magnetron Sputtering Technique", *Nonl. Opt. Quant. Opt.*, 52 (2019) 1-12.
[46] R. Saravanan, **"Novel Ceramic Materials"**, Materials Research Forum LLC (Millersville PA, 2016), Vol. 2, Ch. 4, p. 49.
[47] E.A. Al-Oubidy and F.J. Al-Maliki, "Photocatalytic activity of anatase titanium dioxide nanostructures prepared by reactive magnetron sputtering technique", *Opt. Quantum Electron.*, 51(1-2) (2019) 23.
[48] M. Yarestani et al., "Hydrothermal synthesis of cobalt oxide nanoparticles: Its optical and magnetic properties'', *Iran J. Sci.*, 25(4): 339- 343 (2014)
[49] F.J. Al-Maliki and E.A. Al-Oubidy, "Effect of gas mixing ratio on structural characteristics of titanium dioxide nanostructures synthesized by DC reactive magnetron sputtering", *Physica B: Cond. Matter*, 555 (2019) 18-20.

 ISSN (print) 2958-8960 (online) 3006-6042 Printed in IRAQ